A&A 400, 279–291 (2003)
DOI: 10.1051/0004-6361:20021908

Astronomy & Astrophysics

Long-term spectroscopic monitoring of the Luminous Blue Variable HD 160529⋆

O. Stahl[1], T. Gäng[2], C. Sterken[3], A. Kaufer[4], T. Rivinius[1,4], T. Szeifert[4], and B. Wolf[1]

[1] Landessternwarte Königstuhl, 69117 Heidelberg, Germany
[2] L-3 Communications, NASA/GSFC, Greenbelt, MD 20771, USA
[3] Astronomy Group, Vrije Universiteit Brussel, Pleinlan 2, 1050 Brussels, Belgium
[4] European Southern Observatory, 85748 Garching, Karl-Schwarzschild-Str. 2, Germany

Received 7 November 2002 / Accepted 19 December 2002

Abstract. We have spectroscopically monitored the galactic Luminous Blue Variable HD 160529 and obtained an extensive high-resolution data set that covers the years 1991 to 2002. During this period, the star evolved from an extended photometric minimum phase towards a new visual maximum. In several observing seasons, we covered up to four months with almost daily spectra. Our spectra typically cover most of the visual spectral range with a high spectral resolution ($\lambda/\Delta\lambda \approx 20\,000$ or more). This allows us to investigate the variability in many lines and on many time scales from days to years. We find a correlation between the photospheric He I lines and the brightness of the star, both on a time scale of months and on a time scale of years. The short-term variations are smaller and do not follow the long-term trend, strongly suggesting different physical mechanisms. Metal lines also show both short-term and long-term variations in strength and also a long-term trend in radial velocity. Most of the line-profile variations can be attributed to changing strengths of lines. Propagating features in the line profiles are rarely observed. We find that the mass-loss rate of HD 160529 is almost independent of temperature, i.e. visual brightness.

Key words. stars: individual: HD 160529 – stars: early-type – stars: emission-line, Be – stars: variables: general – stars: mass-loss

1. Introduction

A-type hypergiants and Luminous Blue Variables (LBVs), which often show spectra similar to A-hypergiants, are the visually brightest stars in galaxies. The early A-hypergiant HD 160529, which has long been known to exhibit the spectroscopic signatures of extreme luminosity (Merrill & Burwell 1943), has therefore long been considered as one of the visually brightest stars of the Galaxy, comparable to the brightest stars in external galaxies.

The variability of HD 160529 was already established 30–40 years ago through studies of its variable light and its spectrum at different epochs, which indicated changes in its spectral type. The spectral variability of HD 160529 was studied extensively by Wolf et al. (1974), who found variations of the Balmer line profiles, radial velocity variations with an amplitude of about 40 km s^{-1} and line splitting of some metal lines. Intensity variations of absorption lines of the order of 20% and considerable photometric variations were also found. The light variability was studied and described in detail by Sterken (1977) and Sterken et al. (1991).

HD 160529 was classified as a new galactic LBV by Sterken et al. (1991) due to its brightness decrease of 0.5 mag from 1983 to 1991 and an apparent spectral type change from A9 to B8. Apart from the long-term changes, the authors found pulsation-like variations in their photometric data with a quasi-period of 57 days and peak-to-peak amplitudes of 0.1 mag in b and y, while previous analyses suggested a possible 101.3 day period (Sterken 1981). More recent photometry has been published by Manfroid et al. (1991, 1995) and Sterken et al. (1993, 1995).

From comparison with HD 269662 (= R 110), a close photometric and spectroscopic counterpart of HD 160529 in the Large Magellanic Cloud, Sterken et al. (1991) derived an absolute visual magnitude of $M_V = -8.9$ and a distance of 2.5 kpc. They estimated the stellar parameters characterizing the phase of maximum visual brightness to be $T_{\rm eff} \approx 8\,000$ K, $\log g \approx 0.55$, $R_* \approx 330\,R_\odot$ and $M_* \approx 13\,M_\odot$. The derived mass is in good agreement with the mass determined from evolutionary tracks (Lamers et al. 1998).

Sterken et al. (1991) concluded that HD 160529 is located near the lower luminosity limit of the LBV instability strip and possibly in an evolutionary phase after the Red Supergiant state, i.e. in a post-RSG evolutionary phase.

HD 160529 is of much lower luminosity than more typical LBVs such as AG Car (Stahl et al. 2001) and shows much smaller variations of about 0.5 mag in the visual. According

Send offprint requests to: O. Stahl,
e-mail: O.Stahl@lsw.uni-heidelberg.de

⋆ Based on observations collected at the European Southern Observatory at La Silla, Chile (proposals 69.D-0378, 269.D-5038).

to van Genderen (2001), it is at the low amplitude limit of the "strong-active" S Dor variables. The empirical relation between luminosity and amplitude of LBVs (Wolf 1989) is in agreement with this. According to the period-luminosity relation of Stothers & Chin (1995) a "period" of well above 20 yr would be expected. This is in rough agreement with the light curve published by Sterken et al. (1991).

HD 160529 can be considered an intermediate case between normal supergiants and LBVs. The closest counterpart may be the LBV HD 6884 (= R 40) in the SMC (Szeifert et al. 1993) or the LBV HD 269662 (= R 110) in the LMC (Stahl et al. 1990). The variability of HD 160529 is therefore of interest both in connection with typical LBVs such as AG Car (Stahl et al. 2001) and with normal late B – early A supergiants (Kaufer et al. 1996a,b).

Detailed spectroscopic studies of LBVs, which cover both the short and and long time scales, are still very rare and only available for AG Car (Stahl et al. 2001). Studies of more objects with different physical parameters are needed in order to distinguish the general behaviour of LBVs from peculiarities of single objects.

2. Observations

2.1. Spectroscopy

We have observed HD 160529 with several different echelle spectrographs and several telescopes from 1991, January to 2002, June. We have monitored HD 160529 with high time resolution over a time span of 2–4 months in four successive years, i.e. 1992–1995. In addition, a number of snapshot observations have been taken to extend the total time base covered. The epochs of observations and instruments used are summarized in Table 1.

Most of the observations were obtained with the fiber-linked echelle spectrographs Flash (Mandel 1988) and its modified version Heros (Stahl et al. 1996). These instruments were mainly used at the ESO 50-cm telescope, but for a few shorter runs also at the ESO 1.52-m and 2.2-m telescopes. In the Flash configuration, a setting of the spectrograph was used that allowed the observation of the Hδ and He Iλ6678 lines with one exposure, i.e. the spectral range covered the wavelength range from about 4 050 Å to 6 780 Å. The Flash data have been published on CD-ROM (Stahl et al. 1995). Heros is a modified version of Flash, where a beam splitter is used to divide the beam after the echelle grating into two channels, each with its own cross-disperser, camera and CCD detector. The red channel is identical to the Flash instrument. The two spectral ranges of the Heros configuration cover the range from 3 450 Å to 5 560 Å in the blue channel and from 5 820 Å to 8 620 Å in the red channel. The spectral resolution is about 20 000 for both Flash and Heros. The signal-to-noise ratio (S/N) of our spectra strongly depends on the wavelength and is lowest in the blue spectral range. For HD 160529 we typically used an exposure time of one to two hours for Flash and Heros with the ESO 50-cm telescope. In good conditions, a S/N-ratio of at about 100 is reached in the red spectral range.

Table 1. Summary of the spectroscopic observations of HD 160529.

Instr.	Telescope	Sp.	year
Caspec	ESO 3.6 m	2	1991.08
Flash	ESO 50 cm	62	1992.47–1992.75
Flash	ESO 50 cm, 2.2 m	72	1993.09–1994.41
Flash	ESO 50 cm	55	1994.14–1994.49
Heros	ESO 50 cm	23b/27r	1995.22–1995.42
Ucles	AAT 3.9 m	1	1995.76
Heros	ESO 1.52 m	6	1997.30–1995.32
Feros	ESO 1.52 m	2	1999.53–1999.56
Dfosc	Danish 1.54 m	3	2001.74
Feros	ESO 1.52 m	2	2002.49 52455

Further observations with significantly better S/N and spectral resolution were carried out with Feros (Kaufer et al. 2000) at the ESO 1.52-m telescope between 1999 and 2002. The Feros spectra obtained at the ESO 1.52-m telescope cover the spectral range from about 3 600 Å to 9 200 Å in 39 orders. The spectral resolution of Feros is about 48 000. The S/N depends strongly on wavelength and is highest in the red spectral region. The typical exposure times were about 10 minutes.

In addition, a few spectra have been obtained with the Caspec echelle spectrograph at the 3.6-m ESO telescope and the Ucles echelle spectrograph at the 3.9-m AAT telescope. The Caspec spectra cover the spectral range from 3 800 Å to 5 400 Å with a spectral resolution of about 20 000. With Ucles, observations with three grating positions were obtained and the resulting spectrum covers the total spectral range from 3 600 to 6 880 Å. The spectral resolution is about 50 000.

For all instruments, a built-in high-temperature incandescent lamp and a Th-Ar lamp were used to obtain flat-field and wavelength-calibration exposures, respectively.

In addition, we obtained on Sep. 24, 2001, low resolution spectra (3 Å/pix in the wavelength range from 4 000 to 8 000 Å) with the Dfosc focal reducer spectrograph at the Danish 1.54-m telescope at ESO, La Silla. In this case, a He-Ne lamp was used for the wavelength calibration. The Dfosc data are of much lower resolution than the echelle data and allow to study the equivalent width variations only. Since the spectra were obtained in non-photometric conditions, they can also not be flux-calibrated.

The Ucles spectra were reduced with IRAF. All other spectra were reduced with ESO-Midas. The Caspec spectra were reduced with the standard echelle package of ESO-Midas (Ponz & Brinks 1983). For the Flash and Heros spectra a modified version of this package (Stahl et al. 1993) was used. The Feros package (Stahl et al. 1999), also running within ESO-Midas, was used for the reduction of the Feros spectra. The Dfosc spectra have been reduced with the long-slit package of ESO-Midas.

In the years 1992–1995, the star was observed at least once per week and in some seasons up to once per night. In these runs, the sampling is sufficiently dense to cover variations with time scales of a few days.

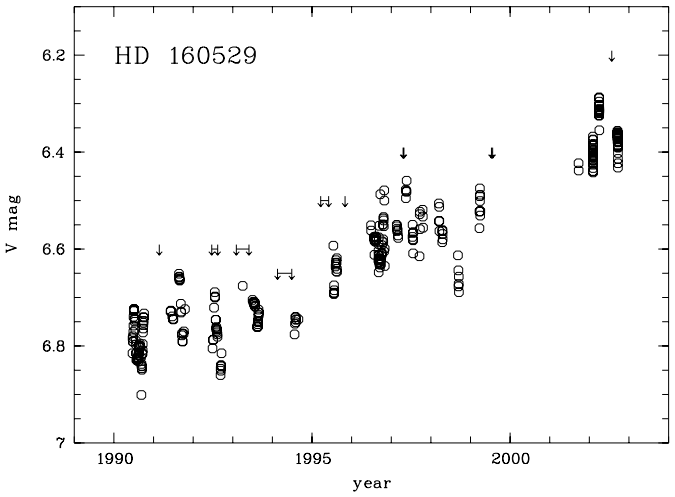

Fig. 1. Results of the photometry of HD 160529 in the Strömgren *y* band. The *x*-axis is in years. The epochs of spectroscopic observations are indicated by arrows, longer observing runs are indicated by double arrows. During our observations, the star evolved from photometric minimum to a new maximum.

2.2. Photometry

Differential photometry was carried out in the framework of the LTPV project (Sterken 1983) using the ESO 50-cm telescope (PMT photometry), the Dutch 90 cm telescope (CCD) and the Danish 1.54-m telescope (CCD) at ESO, La Silla. Zero point corrections were applied but no proper standardization was attempted. The results based on the measurements in the Strömgren *y* band are displayed in Fig. 1.

3. Variability

3.1. Changes in spectral type

The large photometric variations of LBVs are typically accompanied by changes of the spectral type, which can change from Of/WN- to A-hypergiant (Stahl 2001). For HD 160529, spectral types between B8Ia and A9Ia have been published in the literature. However, the spectrum of HD 160529 is peculiar and, since the spectral type depends on the exact classification criteria used, it is not clear if the differences in the published spectroscopic classifications are due to real variations. Most authors find a spectral type of A2–A3 (Wolf et al. 1974), only two authors find a strongly deviating type: Houk (1982) finds A9Ia and Sterken et al. (1991) infer spectral type variations from B8 to A9.

It should be noted, that the spectral types published by Sterken et al. (1991) are not based on spectroscopic criteria, but they are *inferred* from two arguments:

- The observed color variations variations indicate temperature changes from 8 000–10 000 K. This assumes that the theoretical colors apply to the extreme supergiant HD 160529.
- The visual amplitude of 0.5 mag is due to a change in the bolometric correction at constant bolometric luminosity. This assumes that the bolometric corrections (Schmidt-Kaler 1982) for supergiants apply to HD 160529.

The classification (A9Ia) of Houk (1982) is therefore the only spectroscopic classification strongly deviating from the A2–A3 range. The remark of Houk (1982): "H lines seem even weaker than in standards; partly filled in?" seems to indicate that this classification is partly based on the weakness of the Balmer lines, which are indeed influenced by emission.

We therefore re-evaluated the evidence for strong changes in the spectral type of HD 160529. From our spectra we infer only minor changes in spectral type for the spectra obtained until 1999. For this period, we determined the spectral type of HD 160529 by comparing with the supergiant stars β Ori (B8Ia), HD 96919 (B9Ia), HD 92207 (A0Ia) and HD 100262 (A2Ia) from the sample of Kaufer et al. (1997). The match of most lines is reasonably good with an approximate spectral type of A2Ia. The spectral type as determined from the strength of the metal lines is certainly always later than A0 and earlier than A5Ia. Since most of the metal lines are forming partly in the expanding atmosphere of HD 160529, it is not clear how this spectral type relates to the star's effective temperature. This spectral type of A2Ia is in disagreement with the strength of He Iλ5876, which would indicate a spectral type of B9Ia – A2Ia. The given range reflects the strong variations of this line (Fig. 2).

We find that the spectrum before 1999 was significantly different from the maximum phase spectra of Wolf et al. (1974). The spectral type was earlier (hotter) than in maximum phase. In addition, the emission lines are stronger in minimum phase. The temperature change is inferred mainly from the weakening of Ti II and Cr II lines in photometric minimum. However, since these lines form also in the stellar wind, the spectral type changes are unreliable indicators for the effective temperature. The He Iλ5876 line may be a better temperature indicator than the metal lines, although the variable profile of He Iλ5876 indicates that this line is also not of purely photospheric origin.

Nevertheless, part of the spectral changes can certainly be attributed to changes in temperature. The strength of most metal lines strongly increased in 2002. In particular the Ca Iλ4227 line, which had equivalent widths around 50 mÅ in earlier years, increased to about 270 mÅ in 2002 (Fig. 3). This line is a good temperature indicator for A stars. The strength of this line is slightly smaller than in the LBV HD 269662 (= R 110) in 1989, which at that time was classified as about F0Ia (Stahl et al. 1990). The evidence is strong that the star in 2002 was considerably cooler than in the years before. The spectral type was earlier than F0, but much later than A2 and probably late A, confirming the spectral type variations reported earlier.

3.2. Variations of line strengths and radial velocity

Since HD 160529 developed a new S Dor phase during our observing campaign, strong spectroscopic changes are to be expected.

The general appearance of the spectrum of HD 160529 changes very little within one observing season. Much stronger

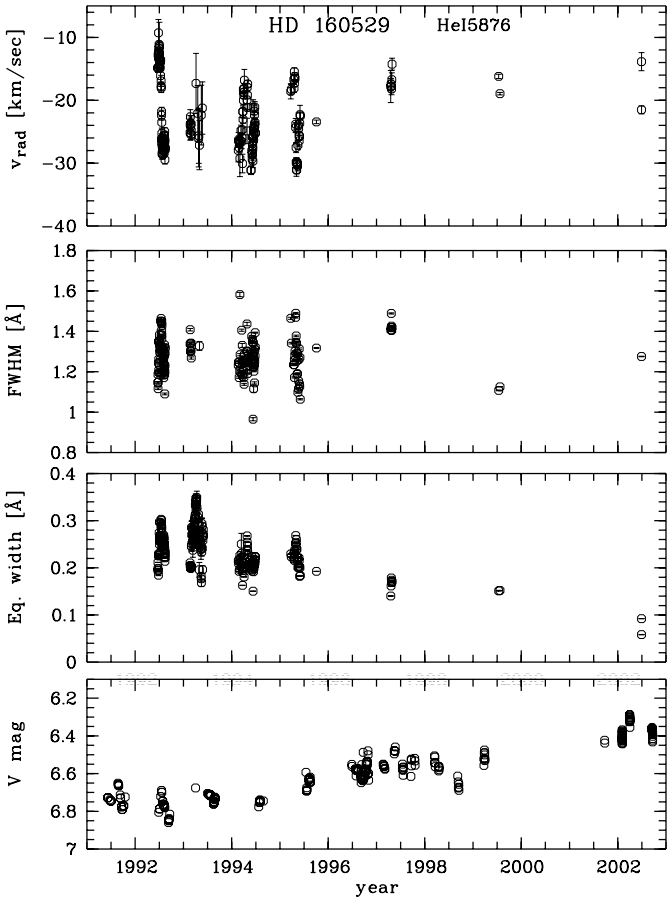

Fig. 2. Radial velocity, FWHM and equivalent width of He Iλ5876 as a function of time. The equivalent width of this line has been measured for other supergiants to 0.68 Å for B8Ia, 0.43 Å for B9Ia, 0.24 Å for A0Ia and 0.10 Å for A2Ia. By this criterion, the star is coolest in 2002.

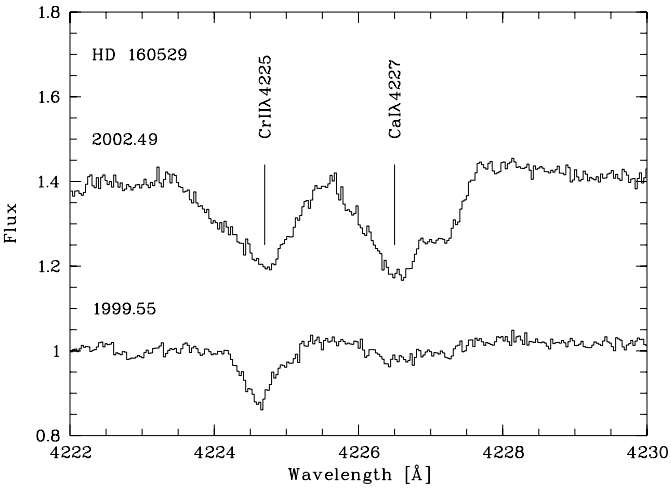

Fig. 3. Variation of the Ca Iλ4227 line. The strength of this line strongly increased in 2002.

variations were observed during the whole campaign from 1992 to 2002. The lines of Cr II and Ti II are very temperature-sensitive in the temperature range of HD 160529 (i.e. about 8 000 to 12 000 K) and temperature changes should be reflected in the *strength* of these lines. Indeed, these lines exhibit

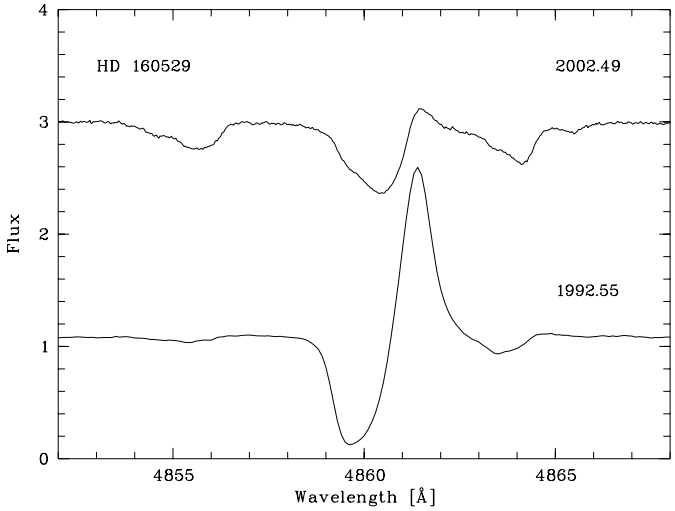

Fig. 4. The Hβ line and two Cr II lines in 1992 (bottom) and 2002 (top). Note the much weaker emission and absorption components of Hβ and the stronger metal absorption lines in 2002 as compared with 1992.

particularly strong variations during our observing campaign. However, the line *profiles* are also highly variable, and is is therefore not clear that the changes in line strength are due to temperature changes only. Especially the short-term changes could be significantly affected by stellar wind effects (cf. e.g. Fig. 7), while the long-term changes, where these effects are averaged out, are more likely to be dominated by temperature variations. Figure 4 shows an example of the spectral changes in Cr II lines. The Cr II are also sharper in 2002, which is also visible when comparing with Fig. 7 of Sterken et al. (1991): they show a spectrum obtained in 1990, where the Cr II lines have a strong blue-shifted component. Compare with Fig. 4 of Wolf et al. (1974), where the Cr II lines are always strong. Also by comparing our equivalent width measurements with Table 6 of Wolf et al. (1974), we find much lower values for Cr II and Ti II in most years. Only in 1999 and 2002, our values approach the values of Wolf et al. (1974). The weakening of Ti II during minimum has also been reported by Sterken et al. (1991).

Figure 4 also shows strong variations of the Hβ line, both in strength and line profile, between 1992 and 2002. The line strength variations are probably caused by a density decrease in the stellar wind, caused by a radius increase and/or a decrease of the stellar radius. The line profile shows that, while the terminal velocity is unchanged, the minimum of the absorption moved to smaller expansion velocities. This could be due to decreased optical depth in the Hβ line or a decrease of the stellar wind velocity in the inner part of the wind.

The He Iλ5876 line is relatively symmetric and thus appears well-suited to study the photospheric variations of HD 160529. The radial velocity of this line is highly variable, but also the FWHM and equivalent width of the line change. We fitted Gaussian profiles to all spectra and so obtained not only the radial velocity but also the residual intensity and line width as a function of time. The results are shown in Figs. 2 and 5. It is obvious from this figure that the line is not only variable in radial velocity but also in line width and intensity. Radial velocity and equivalent width are not correlated.

The equivalent width and radial velocity are highly variable within each observing season, i.e. on time scales of a few months. In addition, the average equivalent width seems to decrease from 1995 to 2002. This probably indicates a lower temperature in these years which is supported by e.g. TiII line measurements. The Hα strength also changed strongly in 1999–2002. The equivalent width was varying between about 14 and 17 Å from 1992 to 1997. In 1999 it was down to 10 Å and further decreased to 7.5 Å in 2001 and to 6.5 Å in 2002.

The relation of spectroscopic behaviour and light curve on short time scales can only be studied from the spectra obtained in 1992, when we have sufficient overlap in the spectroscopic and photometric data set (Fig. 5). The sudden decrease of radial velocity seems to coincide with a peak of the visual brightness. The equivalent width of HeIλ5876 and also the FWHM have a peak at the same time. Note that this correlation of line strength with visual brightness on short time scales contrasts with the pronounced *anti-correlation* on long time scales (Fig. 2). These short-term variations of the HeIλ5876 line could be due to pulsational variations or to stellar-wind effects. If they are due to pulsation, the variations of the equivalent width imply an increase of the temperature with brightness. If we interpret the variations as changes of the stellar wind, the observations would suggest a strengthening of the wind with brightness, with a phase-delay of the radial velocity.

Other lines which mainly originate in the photosphere are e.g. MgIIλ4481 and the SiII$\lambda\lambda$6347, 6371 lines.

If variations in the strength of the TiII, CrII and HeI lines are due to photospheric temperature change of the star, we would expect the changes in HeI and the metal lines to be anti-correlated. Indeed, there is a weak evidence for this behaviour in some years, but the scatter is very large within individual years. In the long-term trend, the anti-correlation is clearly visible.

This is probably due to the fact that the metal lines form mostly in the stellar wind (see Figs. 6 and 7). Only at the end of the observing run, the lines appear close to the systemic velocity and with a line width that is compatible with $v \sin i$. In other years, the radial velocity, line width and line profile variations indicate a stellar wind origin for these lines. Line splitting is quite common and has already been observed by Wolf et al. (1974). In particular in the first years of the observations, the radial velocities are more negative than observed by Wolf et al. (1974) in maximum visual brightness.

3.3. Time series analysis

Lamers et al. (1998) have previously analyzed the photometric data of HD 160529. For two seasons, they derived a period of 45 and 55 days, respectively. They explained the variations by non-radial g-mode pulsations of low order l and the period change by mode-switching.

We examined the photometric data and radial velocity measurements for periodicities with the ESO-Midas TSA package using the method of Scargle (1982). We limited the measurements to seasons with a significant number of measurements. For the photometry, these were the years 1991–1993 and for the

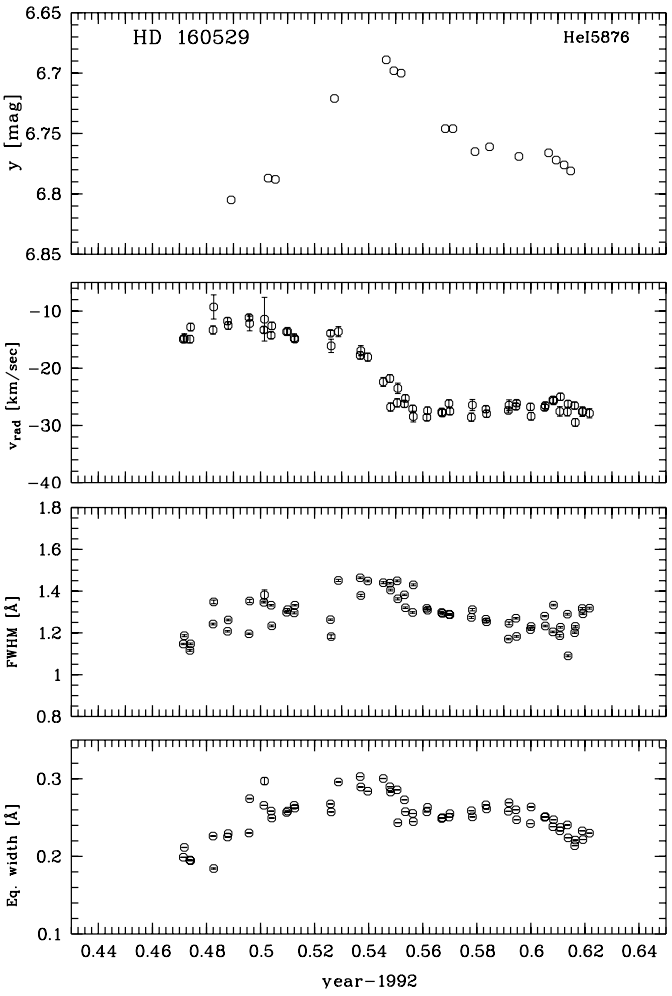

Fig. 5. Photometric and spectroscopic variations of the HeIλ5876 line in 1992. Note the fast changes of almost 15 km s^{-1} within only about 10 days and the relative constancy before and after this change. The equivalent-width curves seems to follow the light curve.

spectroscopy the years 1992–1995. We restricted the search to periods below 120 days, since this is the approximate length of the observing runs. For the y-photometry we obtain the strongest peaks in the power spectrum at about 108, 83 and 68 days and for the radial velocity of HeI at 93 and 67 days. The equivalent width of this line shows two peaks at similar periods at 92 and 67 days and in addition two peaks at 126 and 82 days. We checked that the results do not depend critically on the choice of the data set. If data sets from individual years are removed or added, the detected periods change, but we always find peaks at similar periods, i.e. within a few days. This could indicate that the variations are not strictly periodic or not coherent over longer time scales. However, the small changes of the position of the peaks of the power spectrum are more likely due to the irregular sampling of our data.

It should also be mentioned that the radial velocity changes are definitely not sinusoidal. Although the time series analysis gives time scales of around 100 days, scales for the changes are of the order of 10 days. The time series analysis measures the time scale on which such sudden changes of the radial velocity repeat. Examples of the observed variations are shown in

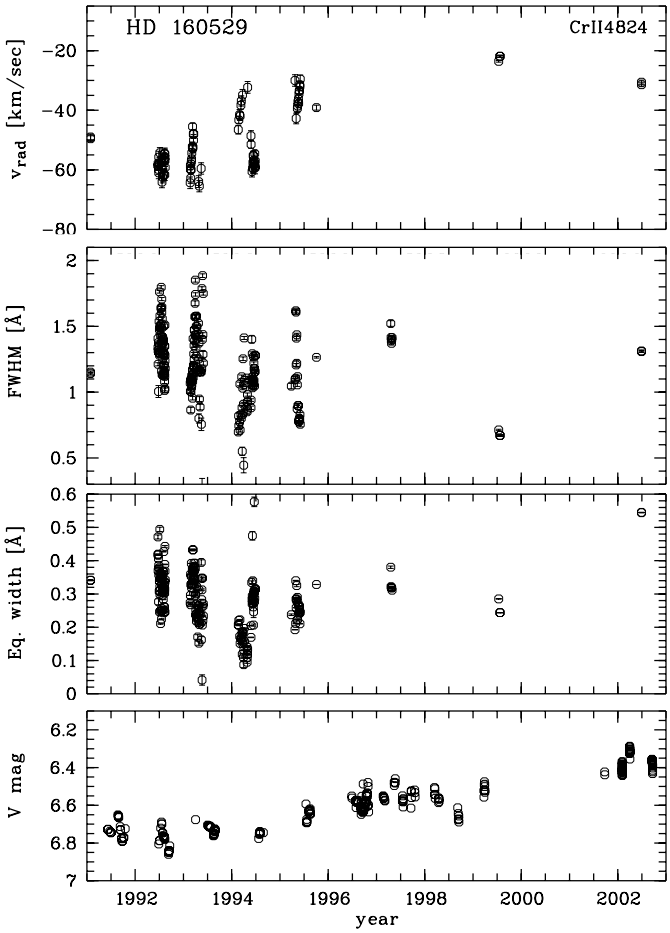

Fig. 6. Radial velocity, FWHM and equivalent width of Cr II λ4824 as a function of time. The parameters have been determined by Gaussian fits to the line profiles, although the line profiles often are not Gaussian. Note the long-term trend in the radial velocity and the extremely strong changes in equivalent width on a time scale of weeks. The average equivalent width of about 0.3 Å indicates a spectral type of about A2Ia, 0.1 Å indicates A0Ia.

Figs. 2 and 5. Similar events have been observed in other years as well.

The similarity between the time scales of the photometric and spectroscopic variations suggests a physical connection. In 1992, when we obtained photometry and spectroscopy almost simultaneously, a peak in the light curve was observed to coincide with the a rapid change in radial velocity (Fig. 5). The equivalent width of He I λ5876 also has a peak at the same time. In fact, the equivalent width seems to follow quite closely the visual light curve. Unfortunately, our observations do only allow to observe these relation in the 1992 observing seasons. Therefore, we can only conclude that the rapid changes in radial velocity *may* be related to the photometric variability.

3.4. Line profile variations

Many lines in the spectrum of HD 160529 show peculiar line profile variations. While this was already known from the work of Wolf et al. (1974), the time sampling of the spectra of these

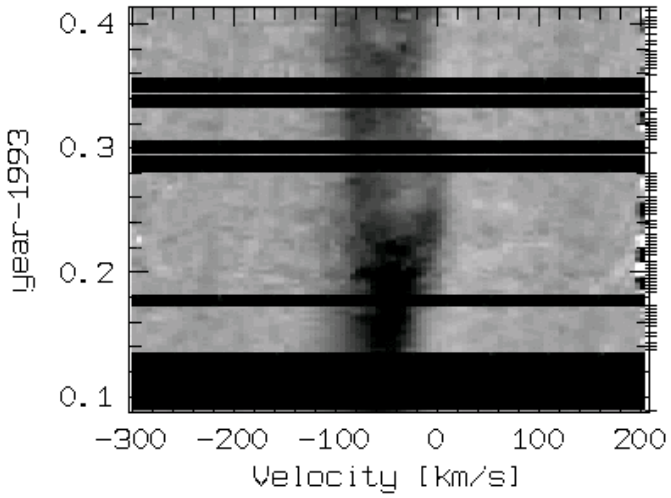

Fig. 7. Profile variations of Cr II λ4824 as a function of time in 1993. Note the strong change in line width and the occasional line-splitting.

authors was not adequate to follow the changes in line profiles in detail.

We searched in particular for propagating features in the line profiles, in order to study the stellar wind of HD 160529. Most of the lines are dominated by absorption and the observed variability seems mainly due to additional absorption. In order to increase the contrast, we therefore examined the residuals of the profiles with respect to a "maximum flux" profile, which was constructed from the time series by computing the highest profile for each wavelength bin in each observing season. This procedure is very sensitive to noise. Therefore, a running median was applied along the *t*-axis before computing the maximum flux. The subtraction of a "maximum flux" profile is more appropriate than subtracting a mean profile if the variations are due to additional absorption on top of a stable profile. The subtraction of a mean profile always introduces emission-like features in the residuals.

A number of strong absorption lines do not show any emission component or a strong wind absorption and, therefore, superficially look like photospheric lines. An example of such metal lines are the Si II lines at 6347, 6371 Å. Profile variations as observed in 1993 are shown in Fig. 8.

Most of the stronger metallic lines, in particular Fe II lines, show pronounced P Cyg profiles. These lines show peculiar variations of the line profiles. An example of the variations is shown in Fig. 10. Also in these profiles, most of the variability can be ascribed to additional absorption of variable strength, but with little change in radial velocity. The variability is strongest at very low velocities around 0 km s^{-1}. This component appears directly on top of the emission component. Therefore the P Cyg profile changes to a splitted absorption profile (Fig. 10, top) and later back to a P Cyg profile. Additional absorption at blue-shifted velocities of about -50 km s^{-1} is also observed, but the features at low and high expansion velocities do not seem to be connected. This second, blue-shifted component seems to move to higher expansion velocities, but the changes are quite small. In some cases, the absorption features even seem to move towards longer

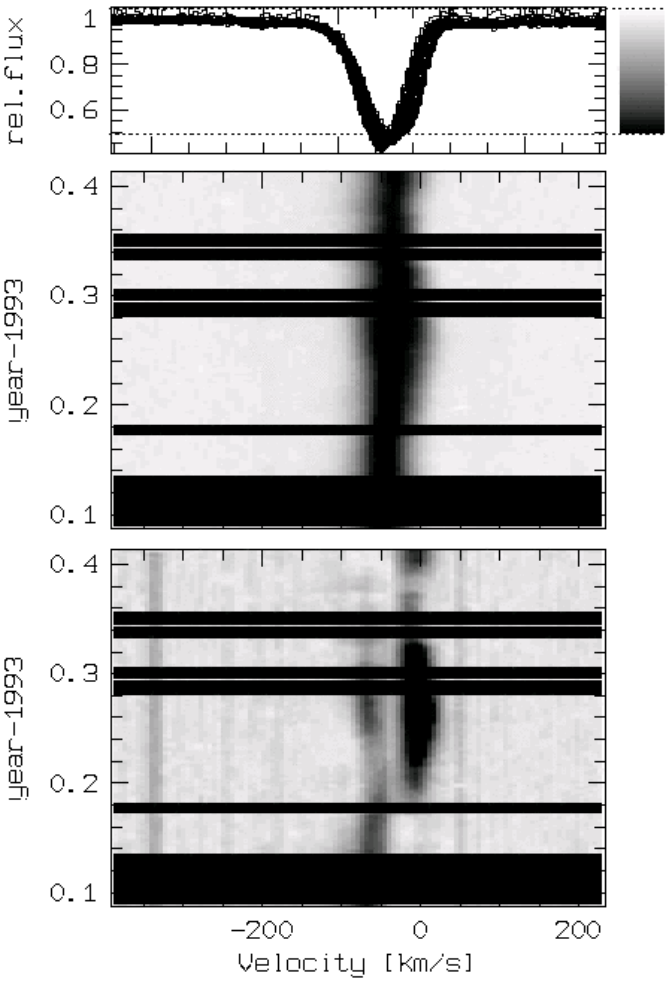

Fig. 8. Profile of the SiIIλ6347 line in 1993. A "maximum flux" profile has been subtracted in the lower panel to enhance the contrast.

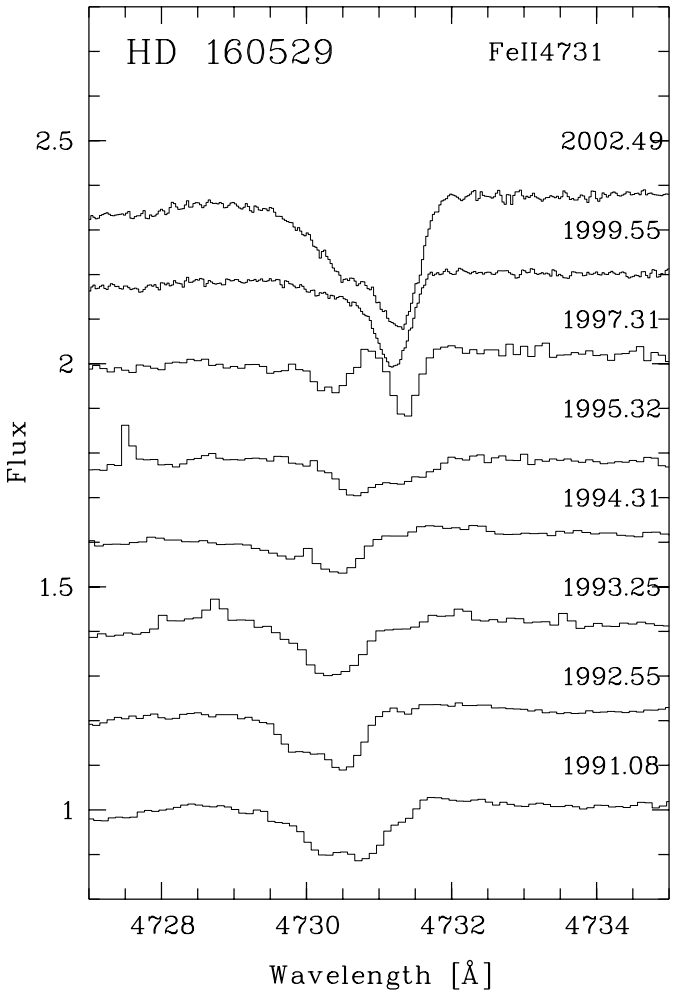

Fig. 9. Profile of the FeIIλ4731 line in various observing seasons from 1991 to 2002. The labels of the spectra denote the date in years. Note the strong low-velocity feature in 1997 and the strength and narrowness of the feature in 1999. In 2002, the strength of the line further increases and a strong blue wing develops.

wavelengths. Features which are clearly moving to higher expansion velocities, i.e. towards shorter wavelengths, are not often observed. Therefore, while we have some evidence for structures which originate in an accelerating stellar wind, the strongest variations occur close to the systemic velocity. A cool photospheric absorption layer may be responsible for these variations.

The low-velocity feature is particularly strong in 1997, where it is clearly seen as a separate absorption feature. As an example we show in Fig. 9 the profile of the FeIIλ4731 line in the various observing seasons. In this figure it can be seen that the line was clearly blue-shifted from 1991 to 1994 and later moved to longer wavelengths. The low-velocity feature could be related to the slightly red-shifted absorption features seen sometimes in LBVs (Wolf & Stahl 1990; Stahl 2001).

A comparison of the line profile variations of lines which have a photospheric appearance (e.g. SiIIλ6347 in Fig. 8) and lines which clearly show a P Cyg profile (e.g. FeIIλ6248 in Fig. 10) shows that the variations are very similar, although the mean profiles of SiIIλ6347 and FeIIλ6248 are very different. It should be mentioned, however, that also the lines with pure absorption profiles show clear variations from year to year in radial velocity and line width.

3.5. The resonance lines NaI, CaII and KI

The NaID lines show, apart from a strong interstellar component, clearly also a stellar contribution: a weak emission component and multiple variable absorption components. The variable absorption components are evidence for accelerating expanding shells. The maximum expansion velocity is typically around -150 km s^{-1} and reaches up to -200 km s^{-1}. Discrete components are frequently observed in the velocity range from -60 to -150 km s^{-1}.

The changes in radial velocity of the components during one observing season are relatively small (up to about about 15 km s^{-1}, but typically below 10 km s^{-1}) The changes from year to year are so large (Fig. 11), that it is not clear how the components are connected from year to year. Therefore, the development of the velocities on longer time-scales cannot reliably be determined from our observations. Similar components may be present at lower velocities as well, but cannot be seen because of the strong interstellar contribution, which saturates the absorption at velocities smaller than about -50 km s^{-1}.

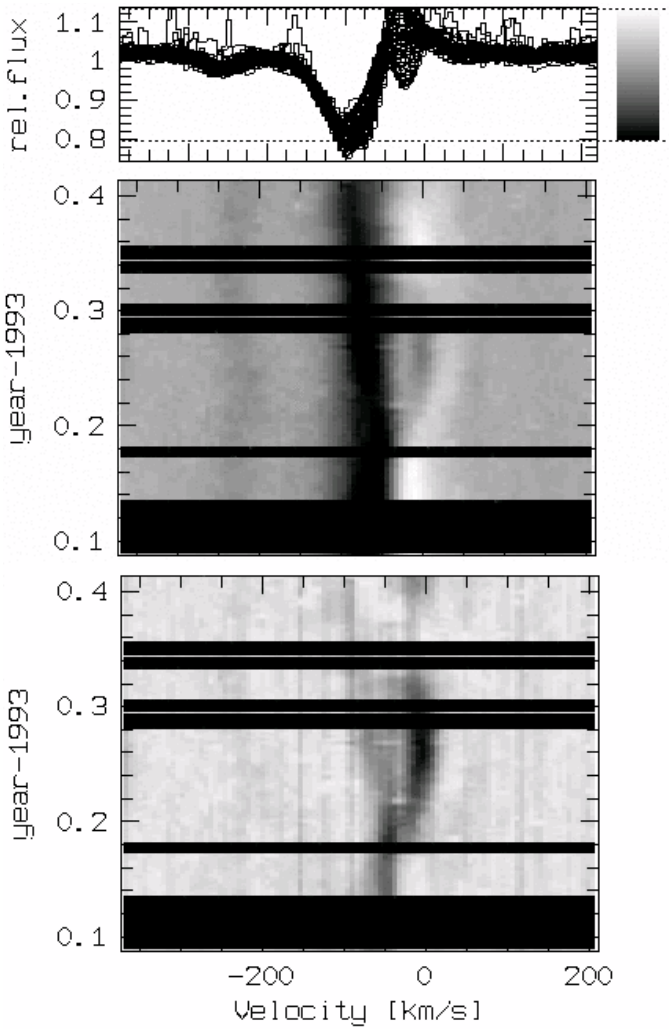

Fig. 10. Profile of the Fe II λ6248 line in 1993. A "maximum flux" profile has been subtracted in the lower panel to enhance the contrast. Note the striking similarity with Fig. 8.

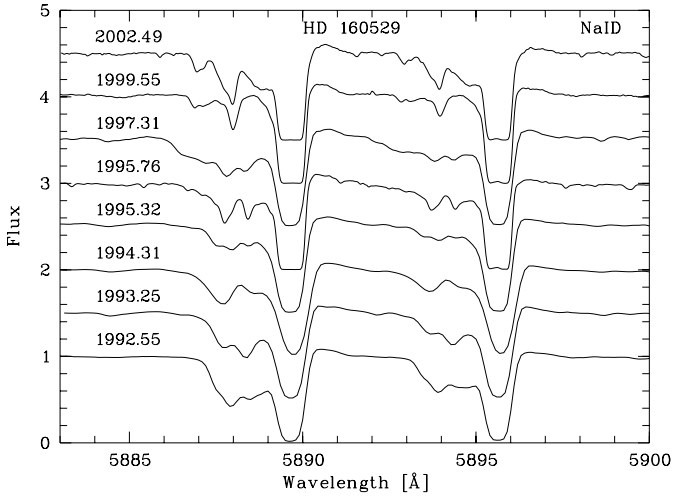

Fig. 11. Mean Na I profiles in the years 1992, 1993, 1994, 1995, 1997, 1999 and 2002. The strongest variations are seen at the blue edge of the absorption component. The spectra are labeled with date in years.

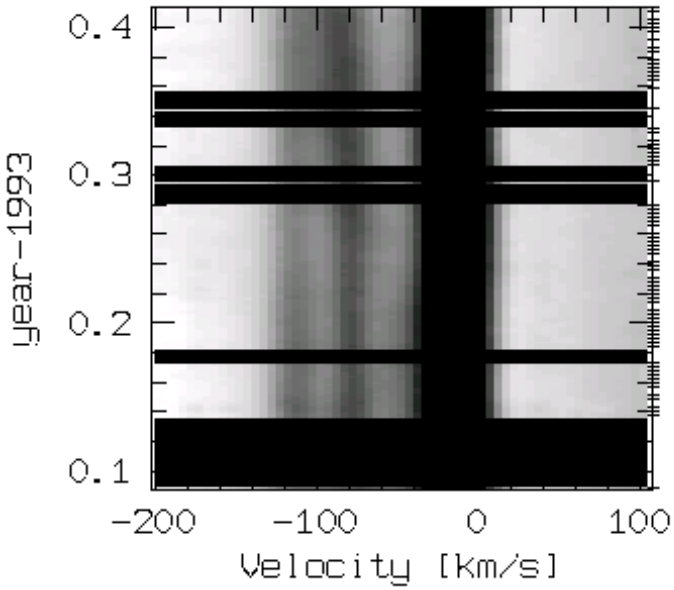

Fig. 12. Dynamic spectrum of Na I λ5889 constructed from the spectra obtained in 1993. Note the accelerating feature around −75 to −90 km s^{-1}. The acceleration of the feature is about 0.12 km s^{-1} d^{-1}.

Acceleration of the components in general is very small. In 1992, no significant acceleration was seen. In 1993 and 1995, an accelerating component was seen, most clearly in 1993 (Fig. 12). Even in this year, we observed an acceleration of about 0.12 km s^{-1} d^{-1} at velocities from −75 to −90 km s^{-1}. Another component at higher velocities (−115 km s^{-1}) was stable in radial velocity. Both components first weakened and later strengthened again. In 1995, three components were observed (−125, −77 and −103 to −114) and one was accelerating. In 1994, two components were seen. Both components were very stable in radial velocity. The component at large expansion velocity (−120 km s^{-1}) was weakening, while the component at smaller velocity (−75 km s^{-1}) was getting stronger with time.

For Ca II H, K much less data is available. In particular, these lines where not covered in the years 1992–1994, where we have obtained the most extended time series. The yearly mean spectra of the Ca II K line are shown in Fig. 13. In cases where both the Ca II and the Na I lines are available, we find different velocities in both groups of lines. The blue-shifted components are much stronger in Ca II and therefore in most cases not as clearly separated. For the un-shifted component, which is mainly of interstellar origin, the Na I lines are stronger than Ca II. In Ca II, the interstellar contribution is split in two components at −26 and −4 km s^{-1}. These components are only resolved in the Ucles and Feros spectra. This splitting is also marginally visible in the Na I lines.

Overall, the picture is not clear. There is no discernible long-term trend in the velocity or acceleration of the components. From an expanding stellar wind (R = 200 $R_\odot$, v_∞ = 200 km s^{-1}, β = 4), the expected acceleration is about 1 km s^{-1} d^{-1}, i.e. significantly larger than what is observed. This implies that the line-splitting is probably not due to radially expanding shells moving with the stellar wind. This behaviour is similar to what is observed for discrete absorption components (DACs) in OB supergiants (cf. e.g.

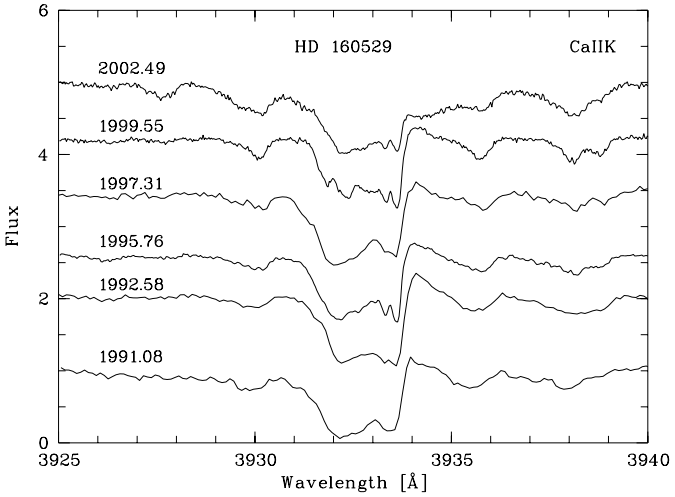

Fig. 13. Mean CaII profiles in the years 1991, 1995, 1997, 1999 and 2002. The strongest variations are seen at the blue edge of the absorption component. The spectra are labeled with date in years.

Fullerton et al. 1997). The origin of these features and their slow acceleration is still not understood.

The KI line at 7699 Å is another interstellar absorption line. This line has only been observed from 1995 to 2002. Due to the low abundance of K, the line is much weaker than NaI or CaII. No blue-shifted components are seen. The line has two absorption components: a strong main component at −2 and a weaker component at −29 km s^{-1}. The components are clearly resolved only in the Feros spectra. From the two Feros spectra it appears that the fainter, blue component is slightly variable and therefore at least partly of stellar origin.

4. Stellar parameters

4.1. Distance

The distance of HD 160529 is important for the derivation of stellar parameters. Unfortunately, the distance is very uncertain: Sterken et al. (1991) estimate a distance of 2.5 kpc based on assigning to HD 160529 the same absolute visual magnitude as the LBV HD 269662 (= R 110) in the LMC ($M_V = -8.9$). R 110 is spectroscopically very similar to HD 160529 and also has a comparable photometric amplitude. In addition, an interstellar extinction of $A_V = 3.4$ mag ($E_{B-V} = 1.1$) is assumed. The empirical relation between luminosity and amplitude of LBVs (Wolf 1989) would give a lower bolometric luminosity of about $M_{\rm Bol} = -8.3$, if we assume an amplitude of 0.5 mag. This would also yield a slightly smaller distance estimate of about 1.9 kpc. If we assume that HD 160529 has an absolute visual brightness of $M_{\rm Bol} = -9.5$, similar to HD 33579, the brightest A hypergiant of the Large Magellanic Cloud, the distance would be 3.5 kpc.

A kinematic distance estimate is difficult for several reasons: the systemic velocity is difficult to determine because of variable radial velocities and line profile variations. In addition, the line-of-sight to HD 160529 is close to the galactic center and kinematic distances therefore have large errors. In the following, we will assume a distance of 2.5 kpc but note that this distance has a rather large uncertainty of about 30%.

4.2. Temperature changes

The temperature of HD 160529 is another uncertain parameter. Line strengths, derived e.g. from SiII, HeI and FeII or TiII give contradictory results, when they are compared to normal supergiants or analyzed with static model atmospheres. This is certainly due to temperature stratification in the expanding atmosphere and stellar wind contributions in most absorption lines.

The only metal which appears in different ionization stages is Mg. The MgI/MgII line ratio can be used to estimate the spectral type. The MgI lines $\lambda\lambda$3832, 3838, 5173, 5183 and the MgII lines $\lambda\lambda$4481, 7877 were used. The results are summarized in Table 2. For comparison, the A0Ia star HD 92207, the A2Ia star HD 100262 and the F3Ia star HD 74180 were also measured. It should be noted that the line profiles of the measured lines also change with time. Therefore, the measured line ratios do not necessarily reflect changes in the effective temperature only. It is likely, however, that most of the variations of the line ratios reflect temperature changes.

The near-IR also contains a large number of NI lines, mainly in the wavelength range around 7 440 and 8 700 Å. These lines are very strong, significantly stronger than in any of the late B/early-A supergiants observed by Przybilla & Butler (2001). For the spectra taken between 1995 and 1999, where the equivalent widths of these lines are relatively stable, we obtain for the lines $\lambda\lambda$7424, 7442, 7468 mean equivalent widths of 325, 417 and 533 mÅ, respectively. In 2002 the lines are still stronger, with equivalent widths of 423, 529 and 614 mÅ, respectively. For HD 100262 (A2Ia), we measure 87, 141 and 196 mÅ, respectively. The latter numbers are in very good agreement with the A2Ia star HD 111613 investigated by Przybilla & Butler (2001). The much stronger lines for HD 160529 may indicate an enhanced abundance of N, but could also be due to non-LTE effects.

Lines from neutral oxygen are strong in HD 160529. We measured an equivalent width of between 2.15 and 2.40 Å for the near-IR triplet $\lambda\lambda$7771-5. For A stars, the strength of this feature increases with decreasing $\log g$ (Przybilla et al. 2000).

In principle, the temperature can also be derived from the continuum energy distribution. The optical energy distribution is not very temperature sensitive, so the UV energy distribution is needed. In the case of HD 160529 this is difficult since the interstellar reddening is high and quite uncertain. However, low dispersion IUE spectra obtained in 1992 and 1979, i.e. during the visual minimum and maximum phase, respectively, show that the flux at about 2 500 Å is *lower* by about a factor 2 in visual maximum. This convincingly demonstrates that the temperature was significantly lower at visual maximum.

We tried to use synthetic spectra computed with the hydrostatic model atmosphere code TLUSTY (Hubeny & Lanz 1995; Lanz & Hubeny 2001) to determine the temperature of HD 160529 and its changes. However, it turned out that the line spectrum of HD 160529 cannot be explained by

Table 2. MgI and MgII equivalent widths in mÅ. Note the strengthening of MgI in 1997 and later. The line ratio MgI/MgII at most times gives a better match with HD 100262 (A2Ia) than with HD 92207 (A0Ia). In 2002, the equivalent widths are exceptionally high and indicate a much later spectral type. The Mg Iλ3832 line is blended in HD 74180.

	MgI				MgII	
season	3832	3838	5173	5183	4481	7877
1992	-	-	61	61	788	-
1993	-	-	64	76	783	-
1994	-	-	71	66	733	-
1995	156	134	89	82	761	149
1997	164	205	137	142	706	127
1999	164	183	116	105	714	201
2002	397	398	378	273	834	268
HD 92207	47	43	25	29	649	104
HD 100262	161	173	124	145	667	194
HD 74180	-	450	553	491	766	220

hydrostatic models. Models with solar abundance which fit the He Iλ5876 line in minimum require about 11 000 K, while fits of metal lines such as, e.g., Mg IIλ4481 would require about 9 000 K. Increasing the He abundance reduces the discrepancy only slightly. We interpret this result as a strong indication of stratification effects in the expanding atmosphere. Non-LTE models which include the atmospheric expansion and line blanketing are required. While such models are now available for WR stars (Hillier & Miller 1998), they are so far not yet available for cooler stars like HD 160529.

The changes of temperature and radius over the variability cycle can be constrained by assuming that the bolometric magnitude of HD 160529 is constant. The change of 0.5 magnitudes in the visual brightness then reflects a change in the bolometric correction. Assuming a minimum temperature of 8 000 K and a corresponding radius of 330 $R_\odot$, we derive a maximum temperature of 12 000 K and a corresponding radius of 150 $R_\odot$. The change of the temperature is necessary for a corresponding change in bolometric correction. This conclusion follows assuming a black-body distribution or if we use empirical bolometric corrections (Schmidt-Kaler 1982). The large change in radius is required by the constancy of the bolometric luminosity. The temperatures correspond to spectral type of about B8 in visual minimum and A9 in visual maximum (Schmidt-Kaler 1982), in agreement with the spectroscopic evidence.

4.3. Systemic velocity and rotational velocity

The systemic velocity of HD 160529 is difficult to determine since all absorption lines are influenced to some extent by the stellar wind, their radial velocities are variable and different for different groups of lines. We therefore selected emission lines which appear little disturbed by absorption to estimate the systemic velocity. The Fe II lines of multiplets 40 and 46 appear well suited. From these lines we derive a radial velocity of -29 ± 3 km s^{-1}. We also used the forbidden line N IIλ6583 to estimate the systemic velocity. This line is flat-topped and probably forms at large distance from the star. The line center, as estimated from the bi-sector of the left and right edge, is at -8 km s^{-1}, if we use a rest wavelength of 6583.454 Å (Spyromilio 1995). Unfortunately, the line is faint and broad, so that the uncertainty of this measurement is large.

The average velocity measured from He Iλ5876 is about -23 km s^{-1} (see below), which is relatively close to this value. Other absorption lines such as the Cr II multiplet 30, which appear as symmetric and narrow absorption lines in maximum, have velocities of around -20 km s^{-1}. The red O I and N I lines give similar results: they vary between -27 and -19 km s^{-1} from 1995 to 2002. Because the radial velocity may be variable also for symmetric lines, it is not clear whether this velocity represents the true systemic velocity of HD 160529.

Because of the variable line profiles, the rotational velocity $v \sin i$ is also difficult to determine for HD 160529. FEROS spectra taken in 1999 and 2002 show particularly narrow absorption lines. We used these spectra to estimate an upper limit for $v \sin i$. For this purpose, we fitted rotational profiles to some metal lines, taking into account the instrumental resolution of the spectrograph, but no other broadening mechanisms of the lines. In this way, we derive a $v \sin i$ value of about 45 km s^{-1}. This has to be considered as an upper limit, since stellar wind effects and other broadening mechanisms are most likely important.

5. Modeling of Hα

Mass-loss rates derived from radio observations are only little model-dependent. HD 160529 is one of the few stellar objects which are bright enough for current radio telescopes. Leitherer et al. (1995) observed the star at 8.64 and 4.80 GHz and found that the measured flux is consistent with thermal emission from an optically thick expanding wind at constant velocity. The authors adopt the spectroscopic distance of d = 2.5 kpc from Sterken et al. (1991), an electron temperature of T_e = 5 000 K for the radio emitting region and a terminal velocity of v_∞ = 180 km s^{-1} to derive a mass-loss rate of $\dot{M} = 10^{-4.87\pm0.24}\, M_\odot\,\mathrm{yr}^{-1}$.

From our observations (Fig. 14), we find that the emission-line flux of HD 160529 was slowly decreasing during our observing period, i.e. with increasing visual brightness. The variations during each season are much smaller than this long-term trend.

In order to quantitatively investigate the mass-loss rate of HD 160529 versus time, we modeled the mean Hα line of the years 1992 and 2002, which show the strongest and weakest Hα emission, respectively. We used the multi-level line-transfer code described by Bastian (1982) and Stahl et al. (1983). A terminal velocity v_∞ of 200 km s^{-1} was used for both minimum and maximum. Note that stellar-wind theory predicts a decrease of v_∞ with decreasing surface gravity, i.e. with increasing visual brightness of LBVs. This is not easily observed in HD 160529, since there are no lines in the optical with a well-defined blue absorption edge. The absorption edge in Hα is variable, but this can also be explained by changes in the optical depth of the wind. A constant wind velocity cannot be excluded from our observations. We used a β-type velocity law with β = 4. A velocity law with such a slow acceleration was

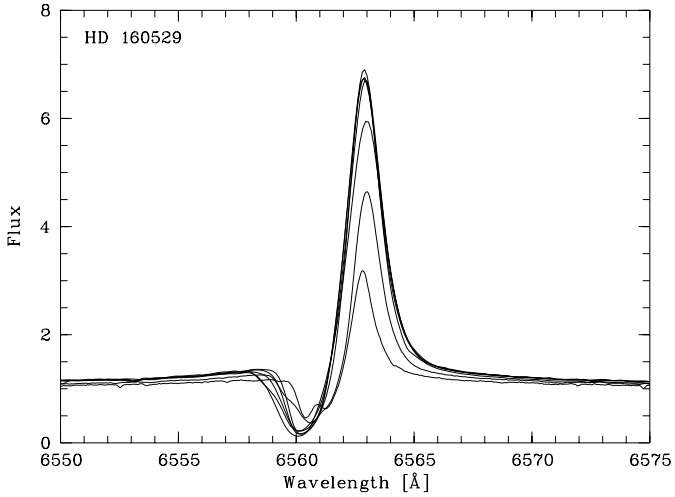

Fig. 14. Mean Hα profile in the years 1992, 1993, 1994, 1995, 1997, 1999 and 2002. In the years 1992–1995, the strongest variations are seen at the blue edge of the absorption component. After 1995, the emission decreased. The weakest emission is present in 2002, the second weakest in 1999.

found by Stahl et al. (2001) to fit the line profiles of AG Car in outburst. The stellar radius and effective temperature were estimated from the photometry and the line spectrum of the given year. Then we only varied $\dot{M}$ and $v_{\rm sys}$ until a satisfactory fit was achieved. Solar abundances were assumed. Possible clumping was not taken into account. The results are summarized in Table 3 and the fits are shown in Fig. 15.

We find that the mass-loss rate of HD 160529 is almost independent of temperature, i.e. visual brightness. Note that the derived mass-loss rate increases slightly from minimum to maximum, although the equivalent width decreases in this period. The reduced equivalent width is mainly due to the radius increase and – to a smaller extent – to the decrease in temperature. The radius increase causes (at constant mass-loss rate) a density decrease which will decrease the equivalent width of the Balmer lines. Therefore, if the radius increase is smaller than derived from the assumption of constant bolometric luminosity, the derived mass-loss rate could even slightly decrease from minimum to maximum. The derived mass-loss rate is in good agreement with the results of Leitherer et al. (1995), which are based on radio observations. We estimate that our mass-loss rates are accurate within about a factor of two. We therefore conclude that within the errors the mass-loss rate did not change significantly between minimum and maximum.

A more advanced modeling of the stellar wind of HD 160529 with a code as e.g. described by Hillier & Miller (1998) would certainly be worthwhile. However, results of such models for cool stars such as HD 160529 are not yet published.

6. Discussion and conclusions

For the interpretation of the short-term variability of HD 160529, the relevant time scales are the rotational time scale $P_{\rm rot}$, the stellar-wind time scale $P_{\rm wind}$ and the pulsation time scale $P_{\rm puls}$.

Table 3. Summary of the mass-loss rate determinations. $v_{\rm sys}$ = -10 km s^{-1} and v_∞ = 200 km s^{-1} where used in both cases.

	min.	max
$R/R_\odot$	150	330
$T_{\rm eff}$/K	12 000	8 000
$M/M_\odot$ yr^{-1}	7×10^{-6}	1×10^{-5}

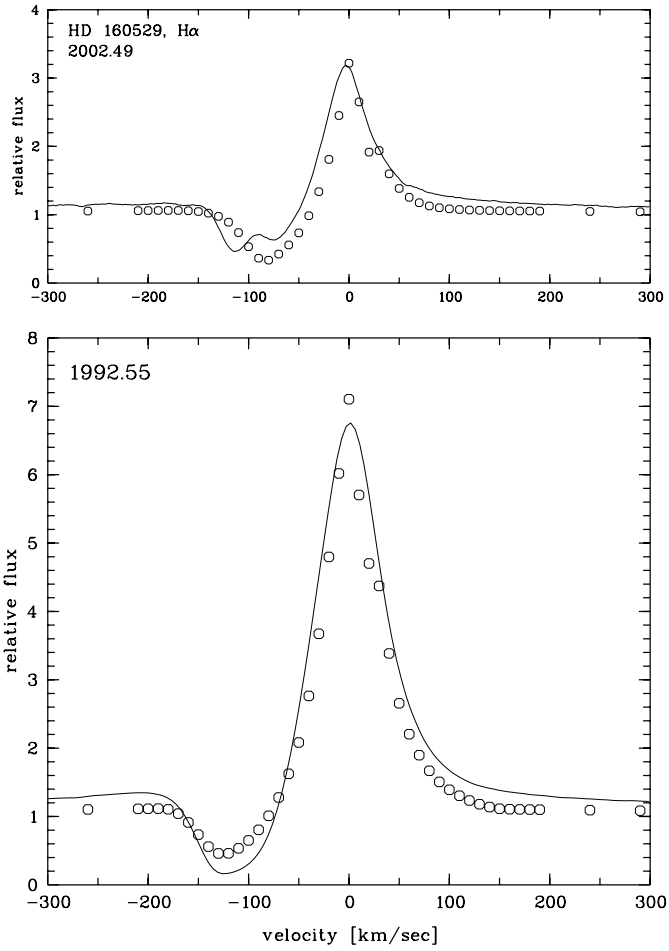

Fig. 15. Fit of the Hα line in 1992 and 2002.

The time scales are defined by the following relations:

$$2\pi R_*/v_{\rm break} < P_{\rm rot} < 2\pi R_*/v_{\rm rot} \quad (1)$$

$$P_{\rm wind} = R_*/v_\infty \quad (2)$$

$$\log P_{\rm puls} = -0.275 M_{\rm Bol} - 3.918 \log T_{\rm eff} + 14.543. \quad (3)$$

In Eq. (1), the upper limit to $P_{\rm rot}$ is estimated from $v \sin i$ assuming $\sin i = 1$. This value can also be slightly larger because the derived $v \sin i$ value is an upper limit. Note that it is expected that the rotational velocity is a function of phase. Because of the complex line profiles it could not be determined in light minimum and is therefore set constant here. Because of the acceleration of the wind to its terminal velocity in the extended stellar wind, the typical expansion time scale can be significantly longer than given by Eq. (2). The pulsation period for

Table 4. Summary of time scale estimates (in days) for the minimum and maximum phase of HD 160529.

	min. (hot)	max. (cool)
$P_{\rm rot}$	59 ... 169	193 ... 371
$P_{\rm wind}$	>6	>13
$P_{\rm puls}$	10	49

the fundamental radial mode given by Eq. (3) is the empirical fitting formula given by Lovy et al. (1984).

We used the following parameters from Sterken et al. (1991): $M_{\rm bol} = -8.9$, $M_* = 13\,M_\odot$. In addition, we used $v_\infty = 200$ km s^{-1} and $v_{\rm rot} = 45$ km s^{-1} for both maximum and minimum phase. For the stellar radius and temperature we adopted 150 $R_\odot$/12 000 K and 330 $R_\odot$/8 000 K for minimum and maximum phase, respectively. With these parameters, we obtain the time scale estimates given in Table 4.

Within the uncertainties, the time scales $P_{\rm wind}$ and $P_{\rm puls}$ are compatible with the typical variation time scales of 50–100 days, while the rotational time scale is significantly longer. However, since rotational modulation can also lead to variations with an integer fraction of the rotational period, the time scale of the variations cannot be used to distinguish the possible mechanisms of the short-term variations in HD 160529. The simultaneous variation of the optical brightness and the He Iλ5876 line, however, is most easily explained by pulsations. Pulsations have also been suggested as a cause for the photometric micro-variations of LBVs (cf. e.g. Lamers et al. 1998).

The correlation of the equivalent width variations with visual brightness on short time scales is in marked contrast with the behaviour on long time scales. This strongly suggests that the physical mechanism for the variations on short time scales is different from the LBV-type variations.

It is rather surprising, that so far no strong dependence of the observed time scale on the visual brightness – and therefore the radius – has been detected. All plausible variability mechanisms would predict such a dependence. It should be mentioned, however, that Sterken et al. (1991) derived a period of 57 days in minimum while the derived value in maximum was 101 days – about a factor of two longer. It is not clear, however, if the difference is due to a real period change.

Most LBVs seem to increase their mass-loss rate in maximum. However, it is not clear that this is a general property of LBVs (Leitherer 1997). Vink & de Koter (2002) have shown that the mass-loss rate of LBVs versus temperature carries important diagnostic information. The mass-loss rate of AG Car versus phase has been studied by Stahl et al. (2001). Vink & de Koter (2002) compared these results with their predictions for line-driven stellar winds and found a good agreement. They also predict that the mass-loss rate of LBVs is a complicated function of temperature, surface gravity and abundances. In particular, the mass-loss rate can even decrease with decreasing temperature at temperatures below about 15 000 K, in particular at low masses. This predicted behaviour nicely fits the observed behaviour of HD 160529, which is an LBV with very low temperature and mass.

Although the mass-loss rates of LBVs can be predicted with some precision, the details of the mass-loss process are still not understood. In particular the complicated line-profile variations and the line splitting cannot be explained by radially expanding features. Rotational modulation may be the cause for these variations.

Acknowledgements. We thank the European Southern Observatory (ESO) for the generous allocation of observing time and the staff at La Silla for the support in the installation of our Heros instrument at the telescope. We acknowledge the use of the SIMBAD database (CNRS data center, Strasbourg). This research has made use of NASA's Astrophysics Data System (ADS) Abstract Service. This work was supported by the Deutsche Forschungsgemeinschaft (Wo 296, 9-1). TG would like to thank C. Leitherer and acknowledges support from STScI-DDRF grants. This project was supported by the Belgian Federal Office for Scientific, Technical and Cultural Affairs (IUAP P5/36), the Belgian Fund for Scientific Research (FWO), and by the Danish Natural Science Research Council, partly through the center for Ground-Based Observational Astronomy. We express our gratitude to T. Arentoft, A. Bruch, H.W. Duerbeck, H. Melief, M. Nolte and A. Visser for contributing some photometric measurements in the framework of LTPV. We thank S. Bagnuolo for taking some of the Feros spectra.

References

Bastian, U. 1982, A&A, 109, 245
Fullerton, A. W., Massa, D. L., Prinja, R. K., Owocki, S. P., & Cranmer, S. R. 1997, A&A, 327, 699
Hillier, D. J., & Miller, D. L. 1998, ApJ, 496, 407
Houk, N. 1982, Catalogue of two-dimensional spectral types for the HD stars, Vol. 3 (Univ. Michigan)
Hubeny, I., & Lanz, T. 1995, ApJ, 439, 875
Kaufer, A., Stahl, O., Tubbesing, S., et al. 2000, in Optical and IR Telescope Instrumentation and Detectors, ed. M. Iye, & A. F. Moorwood, Proc. SPIE, 4008, 459
Kaufer, A., Stahl, O., Wolf, B., et al. 1996b, A&A, 314, 599
Kaufer, A., Stahl, O., Wolf, B., et al. 1996a, A&A, 305, 887
Kaufer, A., Stahl, O., Wolf, B., et al. 1997, A&A, 320, 273
Lamers, H. J. G. L. M., Bastiaanse, M. V., Aerts, C., & Spoon, H. W. W. 1998, A&A, 335, 605
Lanz, T., & Hubeny, I. 2001, in Spectroscopic Challenges of Photoionized Plasmas, ASP Conf. Ser., 247, 351
Leitherer, C. 1997, in Luminous Blue Variables: Massive Stars in Transition, ed. A. Nota, & H. J. G. L. M. Lamers, ASP Conf. Ser., 120, 58
Leitherer, C., Chapman, J. M., & Koribalski, B. 1995, ApJ, 450, 289
Lovy, D., Maeder, A., Noëls, A., & Gabriel, M. 1984, A&A, 133, 307
Mandel, H. 1988, in The impact of very high S/N spectroscopy on stellar physics, ed. G. C. de Strobel, & M. Spite (Kluwer), Proc. IAU Symp., 132, 9
Manfroid, J., Sterken, C., Bruch, A., et al. 1991, A&AS, 87, 481
Manfroid, J., Sterken, C., Cunow, B., et al. 1995, A&AS, 109, 329
Merrill, P. W., & Burwell, C. 1943, ApJ, 98, 153
Ponz, D., & Brinks, E. 1983, The ESO Messenger, 43, 31
Przybilla, N., & Butler, K. 2001, A&A, 379, 955
Przybilla, N., Butler, K., Becker, S. R., Kudritzki, R. P., & Venn, K. A. 2000, A&A, 359, 1085
Scargle, J. D. 1982, ApJ, 263, 835

Schmidt-Kaler, T. 1982, in Landolt-Börnstein, Numerical Data and Functional Relationsips in Science and Technology, ed. K. Schaifers, & H. H. Voigt, Vol. 2b (Berlin: Springer-Verlag), 451
Spyromilio, J. 1995, MNRAS, 227, L59
Stahl, O. 2001, in Eta Carinae and Other Mysterious Stars: the Hidden Opportunities of Emission-Line Spectroscopy, ASP Conf. Ser., 242, 163
Stahl, O., Jankovics, I., Kovács, J., et al. 2001, A&A, 375, 54
Stahl, O., Kaufer, A., Rivinius, T., et al. 1996, A&A, 312, 539
Stahl, O., Kaufer, A., & Tubbesing, S. 1999, in Optical and infrared spectroscopy of circumstellar matter, ASP Conf. Ser., 188, 331
Stahl, O., Kaufer, A., Wolf, B., et al. 1995, Journal Astronomical Data (CD-ROM), 1, 3
Stahl, O., Mandel, H., Wolf, B., et al. 1993, A&AS, 99, 167
Stahl, O., Wolf, B., Klare, G., et al. 1983, A&A, 127, 49
Stahl, O., Wolf, B., Klare, G., Jüttner, A., & Cassatella, A. 1990, A&A, 228, 379
Sterken, C. 1977, A&A, 57, 361
Sterken, C. 1981, in The Most Massive Stars, ESO workshop (ESO), 147
Sterken, C. 1983, ESO Messenger, 33, 10
Sterken, C., Gosset, E., et al., A. J. 1991, A&A, 247, 383
Sterken, C., Manfroid, J., Anton, K., et al. 1993, A&AS, 102, 79
Sterken, C., Manfroid, J., Beele, D., et al. 1995, A&AS, 113, 31
Stothers, R. B., & Chin, C. 1995, ApJ, 451, L61
Szeifert, T., Stahl, O., Wolf, B., et al. 1993, A&A, 280, 508
van Genderen, A. M. 2001, A&A, 366, 508
Vink, J. S., & de Koter, A. 2002, A&A, 393, 543
Wolf, B. 1989, A&A, 217, 87
Wolf, B., Campusano, L., & Sterken, C. 1974, A&A, 36, 87
Wolf, B., & Stahl, O. 1990, A&A, 235, 340